Virchows Arch (1995) 427:131–138

ORIGINAL ARTICLE

Richard E. Tracy

Declining density of intimal smooth muscle cells and age as preconditions for atheronecrosis in the basilar artery

Received: 6 March 1995 / Accepted: 5 April 1995

Abstract The aging basilar artery has some differences and some similarities when compared with the aorta and coronary arteries. As the non-necrotic intimal thickness increases over time, the number of smooth muscle cells reaches a steady state around age 25–30 years in the coronaries and aorta, but continues to increase in the basilar artery, even to 90 years of age. The numbers of cells per unit of tissue (the cell density) declines with age, and the patterns of decline are quantitatively similar in all three arterial segments. All arteries so far examined behave alike in showing that atheronecrosis emerges in those specimens that have sufficiently low density of intimal smooth muscle cells. These results identify low intimal cell density as a criterion for recognizing arteries that are prone to atheronecrosis. One possible explanation is that depopulation of the fibrotically thickened and aged intima, by spreading apart the smooth muscle cells with expanding matrix materials, could be the conditioning factor that brings about the intrusion of atheronecrosis.

Key words Atherosclerosis · Aging · Autopsy · Cerebrovascular disease

Introduction

Atherosclerosis in the intracranial arteries has some similarities and some differences when compared with the disease in the coronary arteries and aorta. In infancy, the internal elastic membrane in the cerebral arteries is of greater prominence than in other arterial systems. The first description of this fact has been attributed to Triepel in 1897 [2]. Intracranial arteries of fetuses and infants demonstrate occasional masses of cellular intima that appear to be associated with defects in the elastica [12]. These developmental defects are thought to be preferential sites of later plaque growth [3, 7]. Most authors have described the growth of plaques as beginning with proliferation of a fibrocellular intima, followed by intrusion of lipid, and later of necrotic cores [1, 2, 4, 8, 10]. As noted in 1966 by Scott et al. [10], "...necrosis does not occur until proliferative lesions reach a minimal thickness roughly twice the medial thickness.... In cerebral arteries, the non-necrotic proliferative lesions seldom become thick enough for an atheroma lesion to develop."

Sometimes a coronary artery or aorta will be found to contain a lipid core of atheronecrosis. This kind of artery often has certain distinguishing characteristics [13, 14, 17]. It typically exhibits fibrotic intimal thickening, extensive lipid deposition as evidenced by foam cell infiltration, and low densities of smooth muscle cells. The aorta requires greater intimal thickening than the coronary artery to produce conditions that favour atheronecrosis. The aorta also requires more extensive foam cell infiltration than the coronary artery. However, smooth muscle cell densities are reduced to equivalent levels in both arterial segments, in company with atheronecrosis. The arteries of different sizes and structures both tend to acquire lipid cores of atheronecrosis when the intimal smooth muscle cell density is equally low. A similar concept has been proposed for intracranial arteries [8]. The depopulation of a fibrotic intima with spreading of the smooth muscle cells apart by expanding matrix materials is under suspicion as a common factor that marks an artery of any size for atheronecrosis.

The present report extends these findings to the basilar artery, as an example of an intracranial artery. Previously reported data on the aorta and coronary arteries are also recalculated for easy use here in comparison with the new findings on the basilar artery.

Materials and methods

The 71 cases providing samples of basilar artery for this series comprise 21 white males, 12 white females, 26 black males and 12 black females, ranging in age from 6 to 92 years. The specimens were obtained in a practice of autopsy pathology, and include subjects from a private hospital as well as forensic cases. Nearly equal

R.E. Tracy (✉)
Department of Pathology, Louisiana State University Medical School, 1901 Perdido Street, New Orleans, LA 70112, USA

numbers of subjects were encountered in the age ranges 36–50, 51–65 and over 65 years; these were matched as needed by subjects less than 36 years of age. All subjects were retained without selection for cause of death, race, sex or other considerations except for age grouping.

Coronary heart disease (CHD) was considered to be the cause of death in 12 cases and cerebrovascular disease (CVD) in 3. In 3 cases, an underlying cause of death could not be determined with certainty. The remaining 53 cases died of conditions that have no known correlation with atherosclerosis, and these are combined into a group that is designated "basal."

The full length of the basilar artery was excised intact from the fresh brain. In many instances an exceptionally large vertebral artery was also retained in continuity and treated as part of the basilar. The specimen was wrapped in filter paper, and immersed in 10% formaldehyde. Thinner arteries became flattened anteroposteriorly during fixation, while thicker ones retained their open cylindrical shape. After fixation and storage for several months, each artery was treated with a decalcifying solution of formic acid-citrate [9], and cut open longitudinally through the middle of the cylinder, whether flattened or round. The cut surfaces of the cylinder, presenting perpendicular aspects of the artery wall for sectioning, were marked with India ink for orientation during embedding. Both halves of the cylinder were treated alike, thereby placing duplicate samples of each arterial segment for evaluation. Paraffin sections cut at 11 μm thickness were stained with haematoxylin and eosin (H & E).

Procedures previously used with the aorta and coronary arteries were applied here to the smaller basilar artery without modification [13, 14]. The entirety of each specimen was scanned, marking with black ink those areas affected by atheronecrosis, and with green ink those areas affected by foam cell infiltrates. The percentage of specimen with atheronecrosis is symbolized "P_A;" the percentage of the non-necrotic specimen affected by foam cells is "P_F." Next, the lengths of the segments of sectioned artery were marked with ink on the cover slip at intervals of 0.5 cm to designate sites for evaluation. At each marked position, intimal thickness and smooth muscle cell numbers were determined. Measurements were made of intimal thickness from luminal surface to intima-media boundary, using an eyepiece ruler calibrated in units of 10 μm. The average of all measurements of fibroplastic intimal thickness is symbolized by "F." The smooth muscle cells were counted within a 100 μm wide band drawn with an eyepiece grid from luminal surface to intima-media boundary. The total number of smooth muscle cells beneath a unit area of endothelium (11×100 μm), averaged over all sites, is called "C_T." Cell density was calculated at each site as cell numbers divided by intimal thickness in units of 100 μm, yielding cells per 10000 μm² of tissue section; averaged over all observations this is "C_D." When the exact position marked for evaluation was unsuitable because of artifactual distortion or other reasons, the nearest suitable position was substituted. The presence of atheronecrosis or foam cells was cause to substitute a nearby position, because smooth muscle cells can be counted only when these dominating features are absent. Descriptive statistics for these variables, including correlation coefficients, are given in Table 1.

The internal elastic membrane in intracranial arteries is conspicuously different from other arteries of the body [2, 4, 8, 12]. Elastin occupies only the outermost zone of the membrane; the inner zones are composed of proteoglycan materials resembling basement membrane or ground substance. Even by H & E staining, the two zones demonstrate different staining qualities (Fig. 1a). Although conspicuous even in childhood, the membrane continues to thicken with age by accretion of ever greater amounts of the inner proteoglycan substances (Fig. 1b–d). Planes of easy dissection within the membrane are made apparent by artifactual tears during preparation of sections (Fig. 1b, c). Eventually, cells appear external or internal to the membrane (Fig. 1e) or within it (Fig. 1d). After a cellular intima develops in later life, the membrane often breaks up and disappears. The internal elastica is treated in this study as a part of the media, and not measured as part of the intima.

Data on the coronary arteries and aorta have been reported at length elsewhere [13, 17], and those reports will not be repeated here. However, some details of those data sets have acquired new uses here for comparison with findings in the basilar artery. Those data sets were therefore retrieved for recalculation to provide the appropriate results for such comparisons. Those arteries were obtained from the International Atherosclerosis Project, and represent several populations from around the world, as well as New Orleans. Moreover, those previously examined specimens were different from the new series of basilar arteries in quality of fixation, long storage in bags of formaldehyde, and in occasional partial drying in the bags. Poor fixation especially was a serious problem; a number of cases were excluded from estimation of smooth muscle cell numbers, because nuclear detail was irregularly demonstrated, a problem never encountered in the basilar artery samples. For these and other reasons, the former data are not strictly comparable to the newly gathered observations. Nevertheless, they offer a first look at the desired comparisons, and are reported here as

Table 1 Descriptive statistics for selected variables in three arterial segments, including correlation coefficients, raw and age-adjusted. raw correlations in upper triangle, age-partialed in lower triangle; (*A* age, *F* thickness, C_T total cell number, C_D cell density, P_F foam cells, P_A atherosclerosis, *SD* standard deviation)

Variable	Units	Number of cases	Mean	SD	Correlation coefficients (*r*)				
					F	C_T	C_D	P_F	P_A
A	Years	71	53.6	19.3	0.67*	0.55*	–0.59*	0.41*	0.41*
F	μm	71	65.4	61.8	–	0.87*	–0.54*	0.39*	0.61*
C_T	Cells	70	7.7	6.3	0.81*	–	–0.27**	0.31*	0.46*
C_D	Cells/10000 μm²	70	14.7	6.3	–0.24**	0.09	–	–0.37*	–0.44*
P_F	%	71	6.5	9.3	0.17	0.10	–0.17	–	0.64*
P_A	%	71	9.0	15.1	0.50*	0.30*	–0.27**	0.57*	–
Coronary arteries									
A	Years	411	44.4	16.1	0.40*	0.25*	–0.23*	0.16	0.35*
F	μm	411	135.3	87.5	–	0.54*	–0.61*	0.55*	0.51*
C_T	Cells	270	15.7	6.6	0.49*	–	0.02	0.19*	0.12
C_D	Cells/10000 μm²	270	15.8	9.2	–0.59*	0.08	–	–0.37*	–0.36*
P_F	%	411	10.2	13.0	0.53*	0.16*	–0.34*	–	0.38*
P_A	%	411	4.9	11.6	0.43*	0.32*	–0.31*	0.35*	–
Aorta									
A	Years	686	44.8	16.3	0.61*	0.16*	–0.60*	0.16*	0.37*
F	μm	686	250.6	165.8	–	0.33*	–0.71*	0.29*	0.65*
C_T	Cells	648	23.0	8.9	0.29*	–	0.03	0.12*	0.03
C_D	Cells/10000 μm²	648	13.8	7.8	–0.54*	0.16*	–	–0.24*	–0.40*
P_F	%	686	23.5	21.1	0.24*	0.09**	–0.24*	–	0.23*
P_A	%	686	5.1	12.1	0.57*	–0.04	–0.24*	0.19*	–

* $P<0.01$, ** $P<0.05$

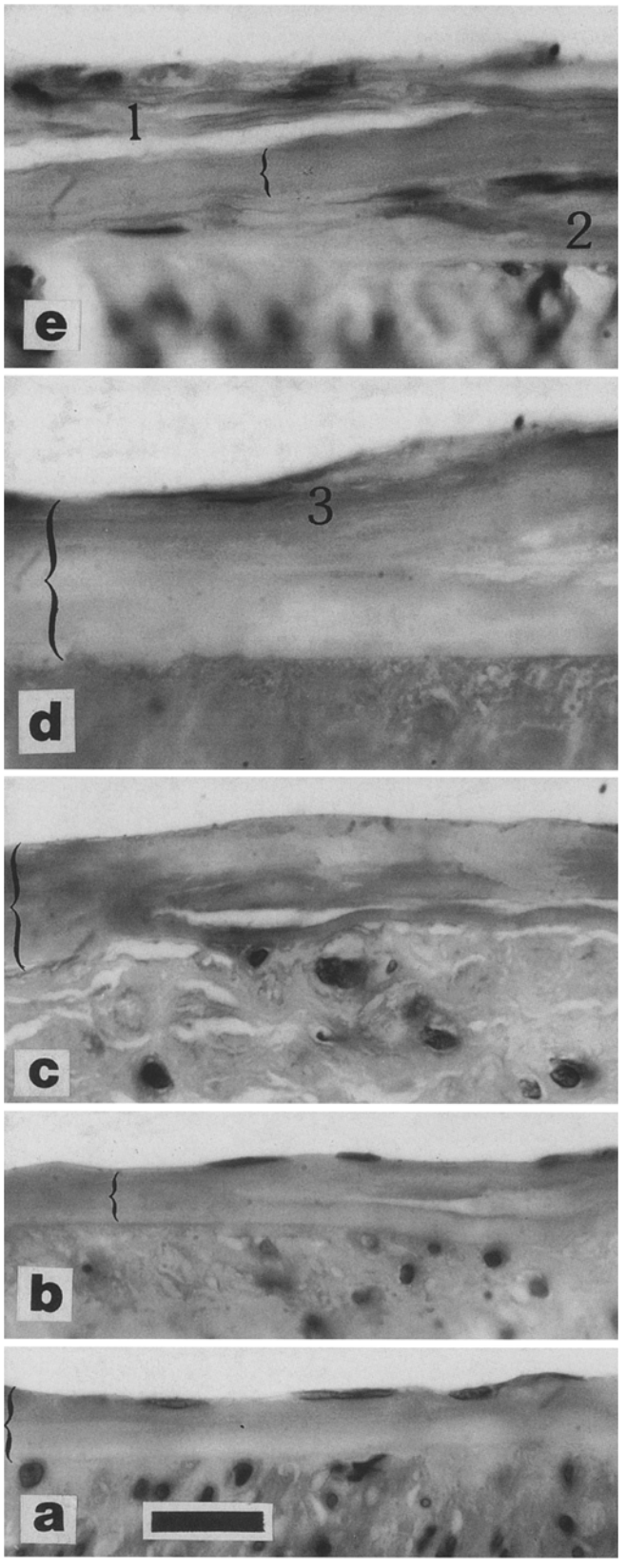

Fig. 1a–e Longitudinal planes through the inner layers of basilar arteries represent commonplace variations in the appearance of internal elastic membrane (*brackets*). When the acellular intima begins to acquire cells, these can be seen interior to (*1*) or exterior to (*2*) the membrane, or within it (*3*). Haematoxylin and eosin (H & E), *bar*=20 μm applies to **a–e**

inconclusive suggestions of what patterns might emerge from future studies.

The interrelationships of several quantitative variables are of interest. Table 1 describes these variables and reports the basic descriptive statistics that are needed for univariate and multivariate analyses. Age is a dominating influence in all circumstances, and cubic regression of each variable on age is used as a way to summarize the relationships; the resulting equations (given in the Appendix) are presented as graphs for easy visualization of the results. The findings of principal interest concern the differences that are found between arteries that do and do not have at least one point of atheronecrosis in the sample ("Yes A" and "No A" specimens, respectively). Discriminant functions offer a way to determine equations that can be used to make such multivariate comparisons. The resulting equations (given in the Appendix) can be set equal to zero, and presented graphically for easy visualization. The resulting plotted curves mark positions on the graphs to use for separating the two classes of specimens. In most instances, the comparisons of interest do not require statistical significance tests, because the observed differences are unequivocal. In those few situations that require significance tests, the appropriate results are reported in the Appendix.

Results

Before 40 years of age, the basilar artery characteristically demonstrates, in most parts of the specimen, an intima that consists of endothelium applied directly to the internal elastic membrane (Fig. 1a–c; in postmortem specimens, the endothelium is often lost to autolysis). The typical specimen, however, does have some sites with cellular substance forming an intima of measurable thickness. The smallest assemblies of cells usually occupy the space interior to the internal elastica (Fig. 2a), although sites of cellularity are sometimes seen within the membrane or exterior to it (Fig. 1d, e). The larger collections of cells are always internal to the elastica, or have no associated elastica, this structure having disappeared, as illustrated in Fig. 2c, d. With increasing age, the intima increases in thickness and numbers of cells (Fig. 2c, d). The increase in intimal bulk is greater for interstitial matrix materials than for cells, separating the cells widely, so that the density of cells declines. At any stage of intimal thickening, foam cells can occasionally be found (Fig. 2e–h), but the likelihood of their presence increases with age and intimal thickness. Atheronecrotic foci are seen in company with thickened intima and greater age (Fig. 2i–k).

The scatter plot (Fig. 3) presents average intimal thicknesses of the non-necrotic points in 71 basilar arteries by age. The lowest of the three solid curved lines represents the regression equation that was fitted to the data. This curve bends upward, illustrating the ever increasing rate of growth of non-necrotic intima. Intimal thickness in the coronary arteries (middle solid curve) is well developed by age 20 years, and increases more slowly thereafter than in the basilar artery. Intimal thickness in the aorta (upper solid surve) shows yet a third pattern, rising steadily from ages 15–55 years.

Basilar arteries having at least one site of atheronecrosis (YesA cases) tend to be older and to show thicker intima in the non-necrotic sites than the specimens having no atheronecrosis (NoA; Fig. 3). In the figure, the

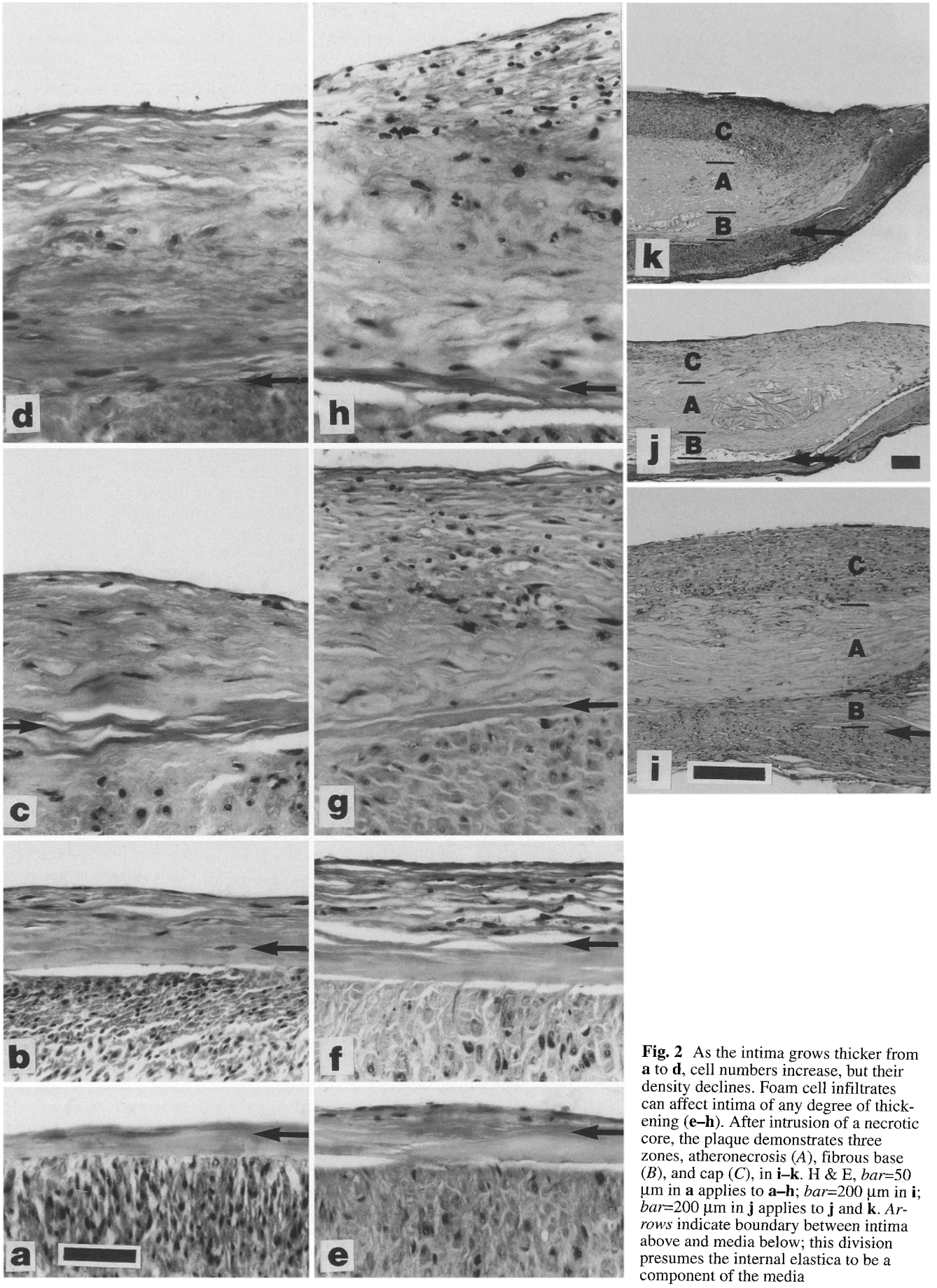

Fig. 2 As the intima grows thicker from **a** to **d**, cell numbers increase, but their density declines. Foam cell infiltrates can affect intima of any degree of thickening (**e–h**). After intrusion of a necrotic core, the plaque demonstrates three zones, atheronecrosis (*A*), fibrous base (*B*), and cap (*C*), in **i–k**. H & E, *bar*=50 μm in **a** applies to **a–h**; *bar*=200 μm in **i**; *bar*=200 μm in **j** applies to **j** and **k**. *Arrows* indicate boundary between intima above and media below; this division presumes the internal elastica to be a component of the media

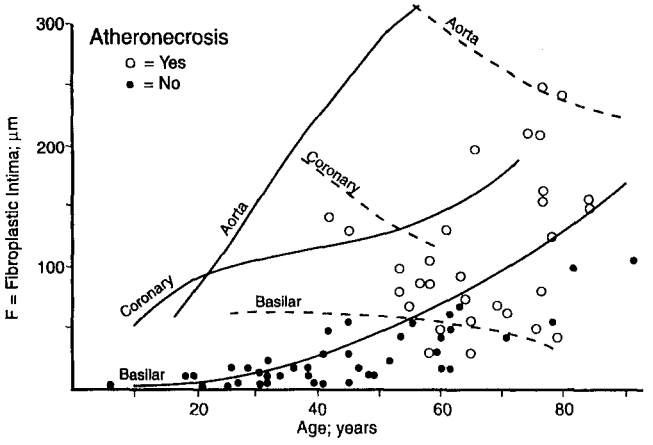

Fig. 3 *Solid curves* represent the cubic regression lines relating fibroplastic intimal thickness to age; *broken curves* represent the optimal location to separate subjects with or without at least one position of atheronecrosis in the specimen. Scatter plots of the data for basilar artery are given. Curves summarizing previously reported data are given for the aorta and coronary arteries

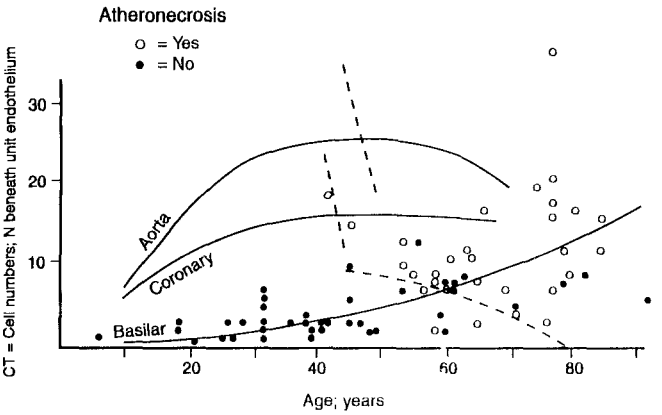

Fig. 4 As in Fig. 3; results for numbers of intimal smooth muscle cells per observed site in each artery

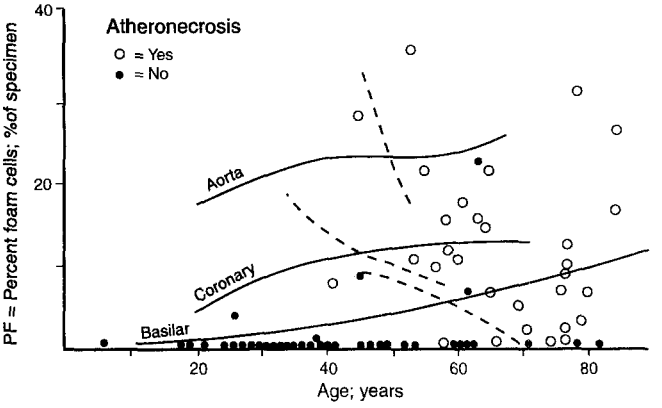

Fig. 5 As in Fig. 3; results for percentage of non-necrotic intima affected by foam cell infiltrates

lowermost of the three broken curved lines represents the optimal place to separate the YesA from the NoA cases. The line is nearly horizontal, because YesA points are above the NoA points, especially at ages 40–60 years; this outcome indicates that intimal thickness is of greater importance than age in relation to the emergence of atheronecrosis. In the coronary arteries (middle broken curve), the threshold for atheronecrosis is at levels of intimal thickness much greater than those in the basilar artery. In the aorta, the threshold for emergence of atheronecrosis (upper broken curve) is at intimal thicknesses nearly six times greater than for the basilar artery.

The lowermost solid curve in Fig. 4 summarizes the scatter of data points on intimal smooth muscle cell numbers and age. This curve reflects the paucity of intimal cells in the basilar artery up to 40 years of age, and the accelerating growth of cell numbers after that age. This pattern contrasts sharply with the middle and upper solid curves which summarize similar results for the coronary arteries and aorta. In those vessels, intimal cells approach their maximal numbers by 25–30 years of age, with little change thereafter.

The lowermost broken curve in Fig. 4 is closer to the horizontal than to the vertical position, because the YesA points are generally above the NoA points, especially at ages 40–60 years; this result illustrates that atheronecrosis in the basilar artery is related more strongly to cell numbers than to age. In sharp contrast to this result, the middle and upper broken curves, which are almost exactly vertical, indicate that cell numbers are of little consequence to the emergence of atheronecrosis in the coronary arteries and aorta, which is dominated, in this chart, by age alone.

The abundance of foam cells increases slowly up to 40 years of age in the basilar artery, but accelerates after that age (Fig. 5, lowermost solid curve). The middle and upper solid curves indicate that foam cell infiltration is nearly maximal in the coronary arteries and aortas by 25–30 years of age, and changes little thereafter. The pattern in Fig. 5 is much like that for smooth muscle cells in Fig. 4, except that the aorta stands out more sharply from the other arterial segments by manifesting much more foam cells infiltration.

The broken curve for the basilar artery is closer to the horizontal than to the vertical position in Fig. 5, because YesA arteries have more foam cells than NoA specimens, especially at 40–60 years of age. The curve for the coronary arteries is positioned above the level for the basilar artery, and the curve for the aorta is still higher, indicating that foam cells are most abundant in the aorta and least in the basilar artery at the boundary between YesA and NoA specimens.

Smooth muscle cell density declines with age in a way that is very similar in all three arterial segments. This result is seen in Fig. 6 by the overlapping of the three solid curves within the same general part of the graph. Unlike the results seen in Figs. 3–5, the differences between arteries in Fig. 6 call for statistical significance tests for their clarification. As detailed in the Appendix, the decline of cell density with age, is significantly different in pattern among the arterial segments ($P<0.001$). However, the magnitudes of the differences are small and could have methodological explanations. Little would be lost by substituting a single equation for all three segments.

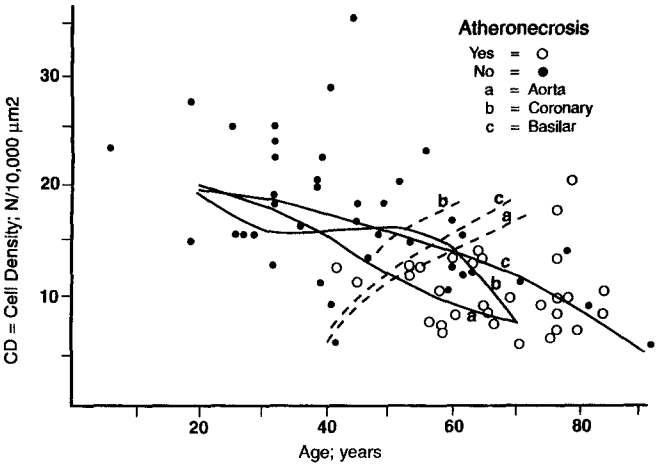

Fig. 6 As Fig. 3; results for density of intimal smooth muscle cells per unit area of tissue section

The broken curve in Fig. 6 represents the basilar artery i.e. curve "c" is more nearly horizontal than vertical; although the YesA points mostly fall to be right of the curve, they also lie generally lower than the NoA points, especially at the 40–60 year ages. This result indicates that YesA arteries tend to be older and, at any particular age, to have lower densities of intimal smooth muscle cells (the statistical significance of this result is documented in the Appendix). The broken curves depicting aorta and coronary arteries are in close proximity to the curve for the basilar artery. Statistical tests show that the differences are not significant (Appendix), and a single line could be substituted for the three separate broken curves of Fig. 6. The pattern indicates that atheronecrosis becomes likely when cell densities drop below a threshold level (about 12 nuclear profiles per 10000 μm^2), but that the threshold is a little higher in old age.

Cell density declines with increasing intimal thickness (solid curves in Fig. 7) and foam cells are likely to affect at least 4% of the sample when the thickness exceeds 60–80 µm in the coronary and basilar arteries, and 10 µm in the aorta (broken curves c, b, and a respectively). Foam cells are likely to affect at least 10% of the specimen when the thickness exceeds 150–170 µm in the coronary and basilar arteries, and 70 µm in the aorta (broken curves f, e and d respectively). Lower cell densities are required in the basilar than in the coronary arteries to favour foam cell infiltration (curve c is below curve b in Fig. 7), and both of these segments are far below the aorta (curve a) in this respect. These thresholds for foam cell infiltration are independent of age and total intimal smooth muscle cell numbers (Appendix).

Table 3 Mean thickness of fibrous cap and base according to thickness of the atheronecrotic core in 176 sites of necrosis found in 71 basilar arteries

Thickness of atheronecrosis (µm)	Fibroplastic thickness (µm)		Number of sites
	cap	base	
1–100	290	50	21
101–200	320	50	55
201–300	330	90	39
301–400	340	90	30
401–500	330	80	13
601–700	330	90	9
701+	350	90	10

Table 2 reports that subjects with CHD or CVD show more intimal thickening and atheronecrosis in the basilar artery than do the basal subjects (those with conditions not known to relate to atherosclerosis). These disease categories do not differ significantly from the basal group in foam cell infiltration, intimal smooth muscle cell numbers or cell density. Race and sex groups did not differ significantly in any of the age-adjusted variables (not tabulated).

The 71 basilar artery samples provided 177 examples of sites affected by atheronecrosis. With increasing thickness of necrotic focus, the thicknesses of the associated fibrous cap and base of the plaques did not change (Table 3).

Discussion

Smooth muscle cells are usually absent from the intima at most sites in the basilar artery at 20–40 years of age. After that age, the numbers of cells, and of affected sites, tend to increase rapidly, although some arteries still show few cells up to the age of 90 years (Fig. 4). Between the ages of 40 and 60, the arteries with the greater numbers of intimal cells often have at least one site affected by atheronecrosis; after 60 years of age, most arteries have atheronecrosis, even when cell numbers are small. This outcome might suggest that increasing numbers of intimal smooth muscle cells act to promote atheronecrosis, since necrosis tends to affect the most cellular arteries. The patterns in the aorta and coronary arteries, however, contradict this suggestion. In these arterial segments, smooth muscle cell numbers reach their steady

Table 2 Means of selected variables measured in the basilar artery, by cause of death, age adjusted (*CHD* coronary heart disease, *CVD* cerebrovascular disease)

Cause	Number of cases	Variable*				
		F	C_T	C_D	P_F	P_A
CHD	12	85A	8.0A	13.0A	9.5A	19A
CVD	3	123A	9.4A	10.7A	13.4A	24A
Basal	53	55B	8.0A	10.8A	5.5A	6B
Uncertain	3	112A	7.5A	15.4A	6.0A	13AB
ANOVA by cause		$F(P)$	$F(P)$	$F(P)$	$F(P)$	$F(P)$
		4.3(0.01)	0.1(0.94)	1.7(0.17)	1.3(0.29)	4.4(0.01)

* Groups within a column sharing a letter, A or B, do not differ significantly ($P<0.05$)

state levels at about 25–30 years of age; later emergence of atheronecrosis is not significantly related to cell numbers. Moreover, necrosis appears in the basilar artery with cell numbers of 4–6 per intimal site, in the coronary arteries with 12–15 cells and in the aorta with 20–25 cells per site. It seems unreasonable that different numbers of cells should be required for necrosis to occur in different arterial segments.

Intimal thickenings increase with age more rapidly than do the numbers of smooth muscle cells, thereby demonstrating a continuing increase in thickness, even after the cell numbers level off (Fig. 3). In all three arterial segments, atheronecrosis is strongly associated with intimal thickness, with greater thickenings required for necrosis in younger than in older subjects. This outcome might suggest that increasing intimal thickness acts to promote atheronecrosis. However, the required thickness is about 300 μm in the aorta, 110 μm in the coronaries and 50 μm in the basilar artery at the age of 55. It seems unreasonable that the various arterial segments should require differing degrees of intimal thickening for the onset of atheronecrosis.

The same considerations arise for foam cell infiltrates. Although atheronecrosis is likely to be found in vessels with more extensive infiltrates, the required amounts vary greatly among arterial segments (Fig. 5). Why should the aorta resist atheronecrosis when affected by far more extensive foam cell involvement than the coronary or basilar arteries? These results suggest that the propensity to retain foam cells is not the primary factor governing the intrusion of atheronecrosis into a location in the arterial tree.

As the density of smooth muscle cells in the intima declines with age, it does so according a pattern that is very nearly the same in all three arterial segments (Fig. 6). Moreover, the likelihood of finding a site of atheronecrosis somewhere in the specimen increases with decreasing cell density according to the same rules in all three arterial segments. These results are consistent with the view that low densities of smooth muscle cells are markers for a predilection to atheronecrosis, and that this predilection is alike in all arteries.

Declining cell densities also increase the likelihood of finding foam cell infiltrates in the non-necrotic intima (Fig. 7). However, the likelihoods vary among arterial segments, even when intimal thickness and cell density are similar. The coronary and basilar arteries resist foam cells more strongly than the aorta. Hence, the declining cell density is not, in itself, the main governor of foam cell deposition at non-necrotic locations. That governor is unidentified. This evidence further argues that atheronecrosis intrudes into a location in the arterial tree for reasons largely unrelated to the reasons for non-necrotic foam cell infiltration. This view is also consistent with data reported by Guyton and Klemp [5, 6], showing chemical and ultrastructural dissimilarities between fatty streaks and necrotic cores.

All arteries so far examined behave alike in showing atheronecrosis to emerge in those specimens that have

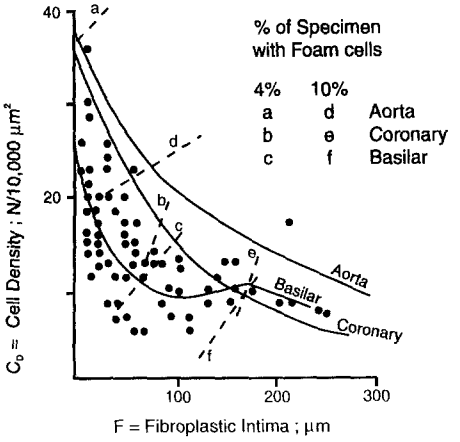

Fig. 7 *Solid curves* represent cubic regression lines relating cell density to intimal fibroplastic thickness; *broken curves* represent the locations that separate subjects with and without specified amounts of foam cell infiltration, whether 4% or 10%

sufficiently low density of intimal smooth muscle cells. The data reported here on the basilar artery agree with those previously reported for the aorta and coronary arteries. These results identify low intimal cell density as a criterion for recognizing the arteries that are prone to atheronecrosis. One possible explanation for these observations is that depopulation of the fibrotically thickened and aged intima, by spreading apart the smooth muscle cells with expanding matrix materials, could itself be the conditioning factor that brings about the intrusion of atheronecrosis. If this simplistic view is correct, then it could further be inferred that the smooth muscle cells may be exerting protective effects upon the interstitial matrix materials, and that atherosclerosis can develop only when these protective influences are impaired. It is also possible, of course, that the low cell density is only a signal of something else that promotes these processes.

Acknowledgements This work was supported by USPHS grants HL-12913, HL-14496, HL-15103 and HL-08974. The photographs were produced by Gene Wolfe and technical help was given by Coralia Lopez and Mary Gandia. We thank J.P. Strong, M.C. Oalmann, W.P. Newman III, H.C. Stary, M.A. Guzman, G.T. Malcom and G.E. Kissling for their cooperative input.

Appendix

Relationship to age (A)

Each of the pathological variables of interest was related to age by cubic regression. Retaining only the significant coefficients ($P<0.05$), and forcing the equation through the origin when the intercept term is not significant, yielded for the basilar artery: $F=0.0203A^2$ ($r^2=0.45$); $C_T=0.00216A^2$ ($r^2=0.27$); $C_D=20.4-0.00178A^2$ ($r^2=0.33$); $P_F=0.00196A^2$ ($r^2=0.18$). The values for the coronary arteries were: $F=7.22A-0.169A^2+0.00154A^3$ ($r^2=0.16$); $C_T=0.661A-0.00618A^2$ ($r^2=0.06$); $C_D=45.4-2.30A+0.0587A^2-0.000481A^3$ ($r^2=0.08$); $P_F=0.431A-0.00385A^2$ ($r^2=0.01$). Those for the thoracic aorta were: $F=0.235A^2-0.00229A^3$ ($r^2=0.35$); $C_T=-6.36+1.43A-0.0153A^2$ ($r^2=0.17$); $C_D=23.3-0.00729A^2+0.0000563A^3$ ($r^2=0.36$); $P_F=1.50A-0.0351A^2+0.000286A^3$ ($r^2=0.04$).

Thresholds for emergence of atheronecrosis

In the evolution of plaques, atheronecrosis is a late change that arises preferentially within a fibroplastically thickened intima [11]. The quantitative details of this evolution, as seen in the coronary arteries and aorta, have been examined at length elsewhere [13–17]. A number of authors have made this observation, in a qualitative way, in studies of intracranial arteries [1–4, 8, 10]. Operationally, the identification of a focus of atheronecrosis somewhere within a specimen indicates that the specimen has made the transformation from the fibroplastic condition (NoA specimens) to the atheronecrotic condition (YesA specimens). The morphometric variables of Table 1, together with age, can be used to distinguish the two classes of cases, the YesA from the NoA, by use of discriminant functions. To accomplish this objective, functions of the form $b_1A+b_2X+b_3AX+C=0$ were determined, allowing the main effects of age (A) and another selected variable (X), and their interactions (AX), into the model. Replacing X in each equation with the selected variable gave these results for the basilar artery (D^2 is the squared distance between means in SD units; % indicates the percentage of cases correctly classified): $0.094A+0.12F-0.0013AF-8.5$ (D^2=5.31, %=87); $0.091A+0.55C_T-0.0047AC_T-7.1$ (D^2=3.52, %=83); $0.083A-0.11C_D-0.0010AC_D-2.3$ (D^2=2.65, %=81); $0.11A+0.48P_F-0.0055AP_F-7.1$ (D^2=3.75, %=86). For the coronary arteries: $0.049A+0.015F+0.00005AF-5.0$ (D^2=2.7, %=80); $0.096A+0.087C_T-0.0015AC_T-4.6$ (D^2=1.13, %=69); $0.14A+0.040C_D-0.004C_D-4.3$ (D^2=2.49, %=79); $0.059A+0.020P_F+0.0021AP_F-4.3$ (D^2=2.80, %=83). For the aorta: $0.00007A+0.0077F+0.00012AF-4.2$ (D^2=3.77, %=85); $0.067A-0.00086C_T+0.00048AC_T-3.7$ (D^2=1.30, %=71); $0.12A+0.087C_D-0.0056AC_D-4.1$ (D^2=2.16, %=77); $0.051A-0.018P_F+0.0012AP_F-3.5$ (D^2=1.84, %=76).

Threshold for foam cell infiltration

The extent of foam cell infiltration was related to selected variables by multiple regression, using a backward stepwise elimination procedure. To place P_F as a dependent variable it was found useful to introduce a square root ($\sqrt{}$) transformation to reduce the severe skewness in the distribution of this variable. $\sqrt{P_F}$ was related to variables A, C_T, C_D, and F (symbols as in Table 1). For the aorta and coronary arteries, the procedure eliminated A and C_T as not statistically significant ($P<0.05$), retaining only F and C_D. For the basilar artery, either A or C_D could be eliminated almost equally well (r=0.244 and 0.254 respectively); to stay consistent with the other arterial segments, an equation retaining F and C_D is therefore appropriate. The resulting equations were $\sqrt{P_F}=0.00971F-0.0760C_D+2.2$ (r^2=0.244) for the basilar artery, $\sqrt{P_F}=0.00980F-0.0462C_D+2.0$ (r^2=0.308) for the coronary arteries, and $\sqrt{P_F}=0.00326F-0.0512C_D+4.1$ (r^2=0.119) for the aorta. These results are given graphically as broken curved lines on plots of C_D by F, representing the cutpoints of $\sqrt{P_F}=2$ and $\sqrt{P_F}=\sqrt{10}$. The graph of C_D by F can be summarized by a regression equation for ease of comparison among the three arterial segments. The cubic relationships serve well: $C_D=23.7-0.32F+0.0024F^2-5.6F^3\cdot10^{-6}$ (r^2=0.464) for the basilar artery, $C_D=36.8-0.29F+0.00096F^2-1.0F^3\cdot10^{-6}$ (r^2=0.511) for the coronary arteries, $C_D=29.9-0.11F+0.00016F^2-8.0F^3\cdot10^{-8}$ (r^2=0.624) for the aorta.

Statistical comparisons between arteries

In most comparisons shown in the graphs, arterial segments are seen to differ distinctly from each other in conspicuous ways that do not require sophisticated significance tests to demonstrate. This is not true for comparisons of cell densities at various ages. Statistical tests were therefore carried out upon the two especially interesting topics. The first involved using cubic regression equations to fit the scatter plots of C_D by A, residual variance attributed to error was calculated for each of the arterial segments, and the sums of squares for error were summed. The sum of squares for error was also calculated for the regression equation that was computed from the whole data set, combining all arterial segments. The pooled sums of squares within segments yielded an estimate of 48.9 for the error variance, compared with 51.6 for the combined data set. The difference is significant ($P<0.001$). The actual magnitude of the effect, however, is small. A single equation derived from the pooled data is $C_D=22.1-0.00566A^2+0.0000416A^3$ (r^2=0.229); this equation has 6% greater residual variance than does the sum of the three separate equations. The second involved calculating discriminant functions for each arterial segment separately to classify cases with or without atheronecrosis, using C_D and A. The numbers of correctly classified subjects totalled 518 (78%). A discriminant function computed for the whole data set, combining all arterial segments, correctly classified 514 cases (77%). Clearly, nothing significant is lost by replacing the three separate equations with the one pooled equation: $0.12A+0.049C_D-0.0041AC_D-3.9$ (D^2=2.15).

References

1. Baker AB, Iannone A (1959) Cerebrovascular disease. I. The large arteries of the circle of Willis. Neurology 9:321–332
2. Blumenthal HT, Handler FP, Blanche JO (1954) The histogenesis of arteriosclerosis of the larger cerebral arteries, with an analysis of the importance of mechanical factors. Am J Med 17:337–347
3. Dahl E (1976) Microscopic observations on cerebral arteries. In: Cervos-Navarro J, et al (eds) The cerebral vessel wall. Raven Press, New York, pp 15–21
4. Flora G, Dahl E, Nelson E (1967) Electron microscopic observations on human intracranial arteries. Arch Neurol 17:162–173
5. Guyton JR, Klemp KF (1993) Transitional features in human atherosclerosis. Intimal thickening, cholesterol clefts, and cell loss in human aortic fatty streaks. Am J Pathol 143:1444–1457
6. Guyton JR, Klemp KF (1994) Development of the atherosclerotic core region. Chemical and ultrastructural analysis of microdissected atherosclerotic lesions from human aorta. Arterioscler Thromb 14:1305–1314
7. Hassler O (1962) Physiological intima cushions in the large cerebral arteries of young individuals. Acta Pathol Scand 55:19–26
8. Klassen AC, Sung JH, Stadlan EM (1968) Histological changes in cerebral arteries with increasing age. J Neuropathol Exp Neurol 27:607–623
9. Lillie RD, Fullmer HM (1976) Histopathologic techniquc and practice of histochemistry, 4th edn. McGraw-Hill, New York
10. Scott RF, Daoud AS, Wortman B, Morrison ES, Jarmolych J (1966) Proliferation and necrosis in coronary and cerebral arteries. J Atheroscl Res 6:499–509
11. Stary HC (1992) Composition and classification of human atherosclerotic lesions. Virchows Arch [A] 421:277–290
12. Stehbens WE (1960) Focal intimal proliferation in the cerebral arteries. Am J Pathol 36:289–294
13. Tracy RE, Kissling GE (1985) Age and fibroplasia as preconditions for atheronecrosis in the human thoracic aorta. Arch Pathol Lab Med 109:651–658
14. Tracy RE, Kissling GE (1987) Age and fibroplasia as preconditions for atheronecrosis in human coronary arteries. Arch Pathol Lab Med 111:957–963
15. Tracy RE, Kissling GE (1988) Comparison of human populations for histologica features of atherosclerosis. Arch Pathol Lab Med 112:1056–1065
16. Tracy RE, Kissling GE, Malcom GT, Devaney K (1987) Sequestration hypothesis of atherosclerosis. Virchows Arch [A] 411:425–434
17. Tracy RE, Kissling GE, Gandia M, Reynolds C (1989) Spatial dispersion of stainable lipid in frozen sections of human aorta. Virchows Arch [A] 415:39–49